Mathematical Geology, Vol. 26, No. 7, 1994

Plio-/Pleistocene Climate Modeling Based on Oxygen Isotope Time Series from Deep-Sea Sediment Cores: The Grassberger-Procaccia Algorithm and Chaotic Climate Systems[1]

Manfred Mudelsee[2] and Karl Stattegger[2]

The question whether paleoclimatic systems are governed by a small number of significant variables (low-dimensional systems) is of importance for modeling such systems. As indicators for global Plio-/Pleistocene climate variability, four marine, sedimentary oxygen isotope time series are analyzed with regard to their dimensionality using a modified Grassberger-Procaccia algorithm. An artificial, low-dimensional chaotic time series (Hénon map) is included for the validation of the method. In order to extract equidistant data the raw data are interpolated with the Akima-subspline method since this method minimizes the change in variance due to the interpolation. The nonlinear least-squares Gauss-Marquardt regression method is used instead of the linear least-squares fit to the logarithmically transformed points, in order to acquire an unbiased estimate of the correlation dimension. The dependences of the estimated correlation dimension on the embedding dimension do not indicate a small number (i.e., less than 5) of influencing variables on the investigated paleoclimatic system, whereas the low dimension for the Hénon map is verified (dimension 1.22–1.28). Because of the limited amount of data in the oxygen isotope records, dimensions greater than about 5 cannot be examined.

KEY WORDS: correlation dimension, interpolation, nonlinear regression.

INTRODUCTION

Plio-/Pleistocene climatic states are commonly deduced from oxygen isotope ratios in oceanic sediments. Frequency spectra of such time series show variance peaks at frequencies corresponding to orbital oscillations ("Milankovitch frequencies," due to variations in eccentricity, obliquity, and precession; e.g., Hays et al., 1976; for reviews see Berger, 1992, and Schwarzacher, 1993). However, the frequency spectra also show a broad range of residual, unexplained variance. On one hand, such spectra can indicate a large number of influencing variables (i.e., noise). On the other hand, as few as three variables,

[1]Received 6 May 1994; accepted 5 July 1994.
[2]Geologisch-Paläontologisches Institut, Olshausenstr. 40–60, D-24098 Kiel, Germany.

interacting nonlinearly, can produce a low-dimensional chaotic time series with such a spectrum (Newhouse et al., 1978; see Schuster, 1989, p. 147–152).

In principle it is possible to distinguish between these two possibilities by applying the Grassberger-Procaccia algorithm (Grassberger and Procaccia, 1983) to the measured time series. However, the validity of conclusions based on the application of this algorithm depends strongly on the quality of the experimental data. In particular, a large number of independent measurements are necessary (e.g., Eckmann and Ruelle, 1992).

The question whether paleoclimatic time series are low-dimensionally chaotic was first investigated by Nicolis and Nicolis (1984) who claimed a dimensionality of about 3 for the upper part of the Pleistocene (0 – ca. 900 ka) climate system. Grassberger (1986) refuted this result. Maasch (1989) investigated 14 oxygen records of about the same time range and concluded a dimensionality in the range 4–6.

In this paper we show the application of the Grassberger-Procaccia algorithm to four Plio-/Pleistocene sedimentary oxygen isotope records probably constituting the largest data sets currently available. As the number of data points is about 3–4 times greater than in the records used in the investigations mentioned above, we expect more precise results. Our data represent climate variability on time scales in the order of 2–5 Ma (late Pliocene global cooling) down to time scales in the order of 3–4 ka.

In the following section the data material is described. We additionally introduce an artificial data set with a known low dimensionality in order to show how its dimension can be estimated by the algorithm. Then the method is described step-by-step. When fitting a power-law curve is necessary, we use nonlinear regression methods, because the commonly practiced method of fitting a linear model to logarithmically transformed points systematically overestimates the inferred exponent of the power-law (Mudelsee and Stattegger, 1994).

DATA

Oxygen isotope ratios ($^{18}O/^{16}O$) are usually written (δ-notation) as parts per thousand (ppt) deviation with respect to a standard sample (e.g., PDB standard). The ^{18}O values from the investigated times series have been measured on planktonic or benthic foraminifera (marine calcareous microfossils). The measurement error ϵ_x is usually about 0.07 ppt (e.g., Tiedemann, 1991). ^{18}O values correspond mainly to the global ice volume and the temperature of the water in which the foraminifera built up their shells. When assuming, reasonably, that the oceanic deep-water temperature is approximately constant in time, one can interpret an oxygen isotope record from benthic foraminifera as a global climate signal. Similarly, when assuming the surface-water temperature of trop-

ical oceans to be constant, one can also interpret an oxygen isotope record, based on tropical living, planktonic foraminifera, as a global climate signal. Because these assumptions may be violated to a greater or lesser degree (Mix, 1992; Seibold and Berger, 1993), we use four cores from different locations and water masses: Deep Sea Drilling Project (DSDP) Site 607 and the Ocean Drilling Program (ODP) Sites 659, 677, and 806 (see Table 1). This strengthens the assumption that we are investigating a global climate behavior, provided that the different cores show similar results. Table 1 shows the characteristics of each investigated oxygen isotope record.

For demonstration purposes, we also investigate an artificial time series generated by the Hénon map (Hénon, 1976). This time series is known to have a low dimensionality (Grassberger and Procaccia, 1983). We use a set of 1000 points (Fig. 1E), thus comparable with the data sizes of the isotope records. The original time series are shown in Fig. 1.

Table 1. Experimental Time Series from the Oxygen Isotope Records Used in this Study

	Location	Water depth [m]	Habitat	T^a (ka)	N^b	$\langle \Delta t \rangle^c$ (ka)	References (#: 18-O data, *: timescale)
DSDP 607	41°N, 33°W	3427	benth.	3040	822	3.7	# Ruddiman et al., 1989 # Raymo et al., 1989 # Raymo, 1992 * Raymo (pers. comm.)[d]
ODP 659	18°N, 21°W	3070	benth.	5268	1194	4.4	# Tiedemann, 1991 * Tiedemann et al., 1994
ODP 677	1°N, 83°W	3461	benth.	3190	1168	2.7	# Shackleton and Hall, 1989; * Shackleton et al., 1990
ODP 806	0°, 159°E	2520	plankt.	2120	531	4.0	# Berger et al., 1993 * Berger et al., 1994[e]

[a] Time range.
[b] Number of data points.
[c] Average spacing.
[d] This timescale is based on that of Shackleton et al. (1990).
[e] Equidistant timescale.

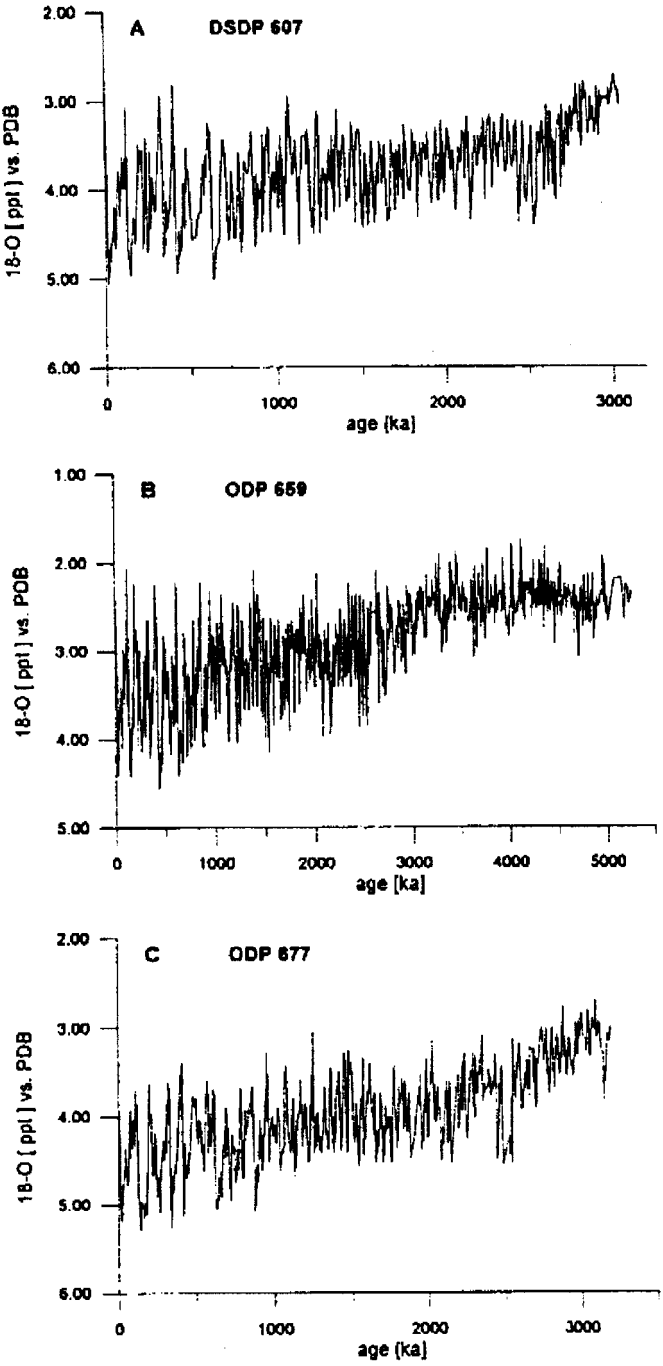

Fig. 1. (A-D) Raw data of the investigated experimental time series (cf. Table 1). The y-axis is inverted according to the conventional representation of cooler (higher ^{18}O values) and warmer (lower ^{18}O values) climatic states. (E) The chaotic Hénon map time series is described by the equation $X(i + 1) = 1 + aX(i)^2 + bX(i - 1)$ with $a = 1.4$, $b = 0.3$. We discarded the first 5000 iterations to eliminate transients to the chaotic state (e.g., Ding et al., 1993) and used as time series $X(5001), \ldots, X(6000)$. Only 500 points are plotted: $X(5001), X(5003), \ldots, X(5999)$.

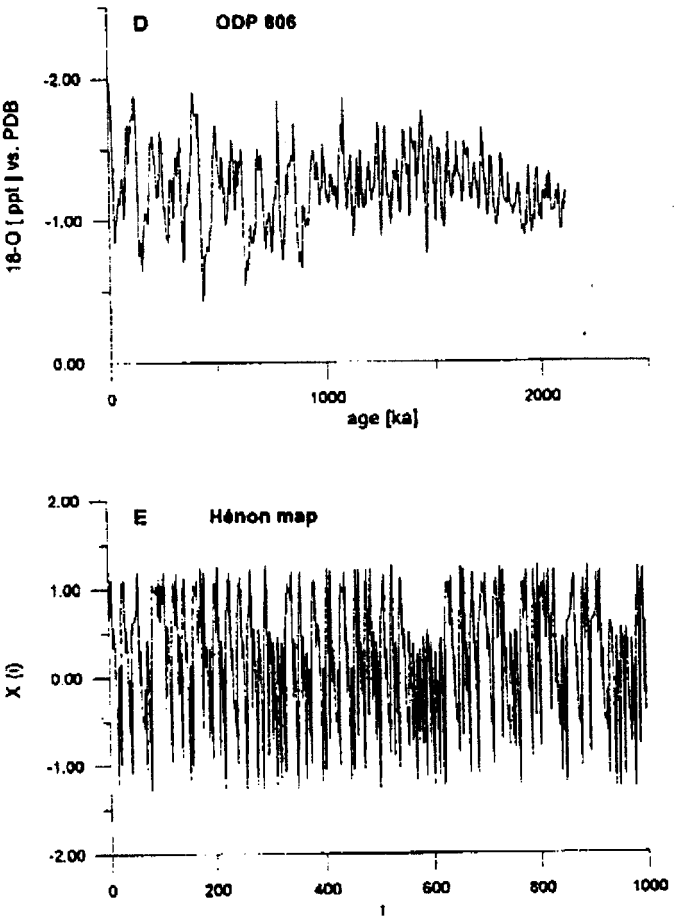

Fig. 1. Continued.

METHOD

Interpolation

As the Grassberger-Procaccia algorithm demands equidistant data, three time series (DSDP 607, ODP 659, ODP 677) must be interpolated. We tried three different interpolation methods in order to find a solution that minimizes the distortion of the total information contained in the time series. We find (Table 2) that the linear interpolation reduces information, whereas the natural cubic spline interpolation strongly generates additional variance. We choose (Table 2) the Akima-subspline interpolation as it is described in Engeln-Müllges and Reutter (1993, Chapter 13): interpolating with polynomials of order less than or equal to 3 and demanding only the first derivative (and the function itself) to be continuous. These findings are in accordance with those of Schulz (1994).

We hold the number of equidistant points generated equal to the number of original data points in order not to enhance the statistical dependence between the points introduced by the interpolation (see Eckmann and Ruelle, 1992).

Table 2. Behavior of the Variances of the Time Series Due to the Interpolation

	Original variance	Δ (Variance)		
		Linear	Cubic	Akima
DSDP 607	3.778	−1.86%	+9.3%	+1.86%
ODP 659	2.888	−5.28%	+16.9%	−0.35%
ODP 677	3.970	−1.54%	+25.1%	+2.32%

Autocorrelation Function

The second preliminary examination, before applying the algorithm itself, consists of determining a typical length of time τ over which two points of the time series, $X(t)$ and $X(t + \tau)$, become linearly independent. As, e.g., Maasch (1989), we use for τ the first zero crossing of the autocorrelation function (Fig. 2), which is calculated after linearly detrending the time series. Three time series (see Figs. 2A, 2B, 2D) give a τ of about 20 ka corresponding to delay of about 5 data points. Concerning the autocorrelation function for the ODP 677 time series (Fig. 2C) we choose the first minimum ($\approx$27 ka) instead of the first zero crossing ($\approx$52 ka) for consistency, indicated by visually comparing the different plots. For the Hénon map time series we choose $\tau = 1$.

Grassberger-Procaccia Algorithm

The Grassberger-Procaccia algorithm uses an equidistant time series,

$$X(1), X(2), \ldots, X(N),$$

with constant spacing and N data points, to construct an M-dimensional space ("embedding space") by means of the p Y vectors:

$$Y(1) = [X(1), X(1 + L), X(1 + 2L), \ldots, X(1 + (M - 1)L)]$$

$$Y(2) = [X(2), X(2 + L), X(2 + 2L), \ldots, X(2 + (M - 1)L)]$$

$$Y(p) = [X(p), X(p + L), X(p + 2L), \ldots, X(p + (M - 1)L)]$$

L denotes time lag (measured in units of the data spacing) and corresponds to τ. For the time series DSDP 607, ODP 659, ODP 677, ODP 806, and the Hénon map time series we use $L = 5$, $L = 5$, $L = 10$, $L = 5$, and $L = 1$, respectively (Fig. 2). Notice that the number p of vectors is given by $N - (M - 1)L$. The embedding space is a reconstruction of the original (unknown) phase space of the investigated system (Packard et al., 1980; Ruelle, 1981). Each vector Y corresponds to a point in the embedding space and reconstructs a specific state of the system, which is described by the time series.

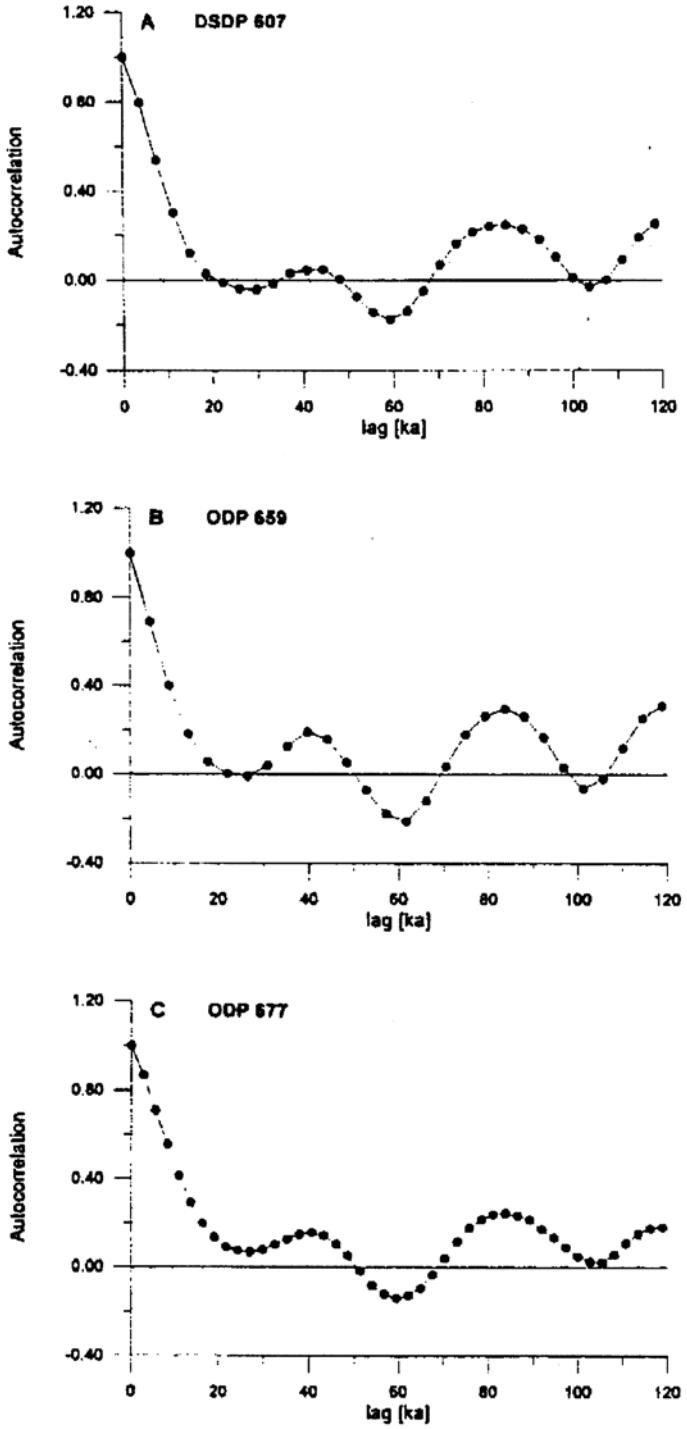

Fig. 2. Autocorrelation functions of the investigated time series.

Next, the correlation integral, $C(r)$, is introduced:

$$C(r) = \text{factor} \times \text{sum of distances } \|Y(i) - Y(j)\| \text{ smaller than } r$$

For the calculation of the distances we use the maximum norm, as recommended

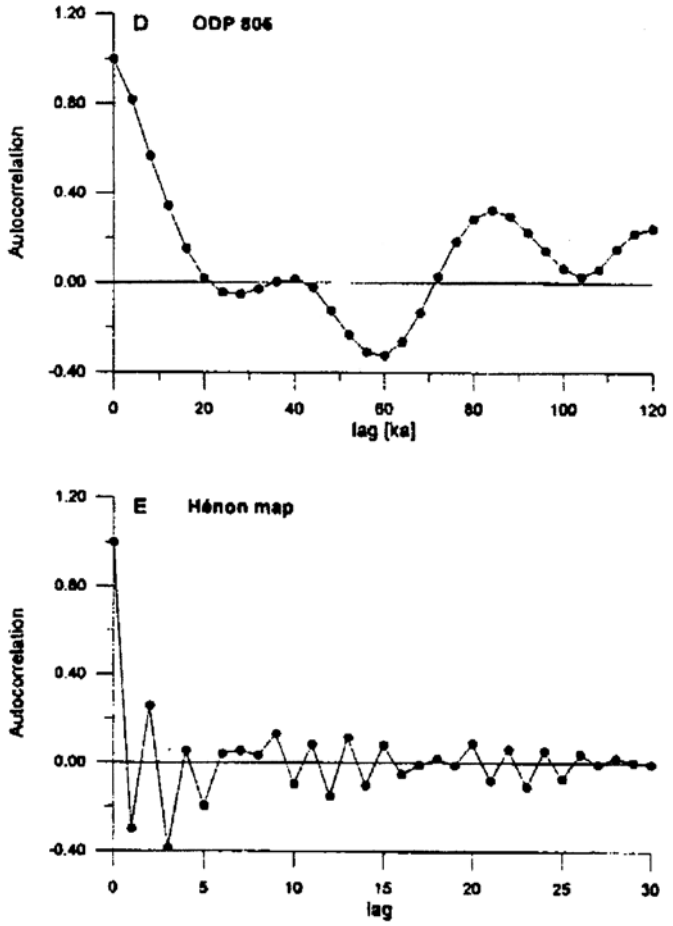

Fig. 2. Continued.

by, e.g., Grassberger (1987). In order to exclude distances between mutually statistically dependent vectors, $Y(i)$ and $Y(j)$, we use the restriction $|i - j| > L$ (Theiler, 1986). The normalizing factor is set equal to $1/[p(p - 1)]$. We also normalize the distances, setting the maximum value equal to one. Notice that due to the symmetry in i and j only about 50% of all distances need to be calculated explicitly.

Grassberger and Procaccia (1983) showed that in the original phase space (of which the coordinate axes are given by the individual influencing variables) of a chaotic system the following relation holds true for small r:

$$C(r) \alpha r^{D_2} \tag{1}$$

where D_2 is the correlation dimension. The correlation dimension does not have to be an integer number. In the embedding space with embedding dimension M, $D_2(M)$ estimates D_2. When M is large enough, the original phase space should be sufficiently well reconstructed and $D_2(M)$ should asymptotically approach a saturation value, $D_{2,\mathrm{sat}}$. Then $D_{2,\mathrm{sat}}$ is taken as the estimate of the correlation dimension D_2. Ding et al. (1993) showed that "large enough" means

$M = \text{Ceil}(D_2)$ with Ceil(z) being the smallest integer greater than or equal to the real number z. But, as they showed, this result only holds true for data sizes $N \to \infty$ and measurement errors $\epsilon \to 0$. Because of this, for experimental time series ($N < \infty$, $\epsilon > 0$), it may happen that the original phase space cannot be reconstructed, i.e. no saturation behavior of $D_2(M)$ is observed. The general dependence of $C(r)$ and $D_2(M)$ for experimental time series is demonstrated by Ding et al. (1993). Ben-Mizrachi et al. (1984) gave guidelines concerning the existence of measurement errors. Eckmann and Ruelle (1992) gave a maximum sensible value of $D_2(M)$ that can be calculated with N data points.

We now proceed as follows: First, we calculate the correlation integrals for $M = 1, 2, 3, \ldots$ (Fig. 3). Then, from $C(r)$ we estimate $D_2(M)$. Our method for doing this is described in the next subsection, along with our findings concerning the influence of the measurement error ϵ_r. The following subsection shows how and up to which value of M we decide to calculate $C(r)$. This value, as mentioned above, depends on N. The final subsection shows how some stochastic time series can be distinguished from low-dimensional chaotic time series.

Estimating the Correlation Dimension by Nonlinear Regression

Estimation of $D_2(M)$ from the power-law relation (Eq. 1) is usually carried out by linear least-squares fitting to logarithmically transformed points (r, C) and taking the slope as an estimate of $D_2(M)$. However, assuming the error of a distance, ϵ_r, to be normally distributed $\sim N(0, \sigma^2)$, as may be required for a specific distance $\|Y(i) - Y(j)\|$, the appropriate regression model for least-squares fitting of Eq. (1) becomes

$$r = aC^{1/D_2} \pm \epsilon_r$$

introducing the second fit parameter, a. We use this model. When its basic assumption holds true, the Gauss-Markov condition $\langle \epsilon \rangle = 0$ would be violated in the double-log model, thus leading to a biased estimation (e.g., Seber and Wild, 1989). Mudelsee and Stattegger (1994) showed that this bias would result in an overestimation of $D_2(M)$. This is also confirmed in the present study (Fig. 4E).

In accordance with the above statement, the power-law dependence (Eq. 1) of the correlation integrals from our time series holds only for small r (Fig. 3). On the other hand, if r approaches the strength of the experimental noise, the points (r, C) become unreliable. The fit region therefore has an upper bound, r_U, and a lower bound, r_L. Our choice of the proper fit region is guided by four aims:

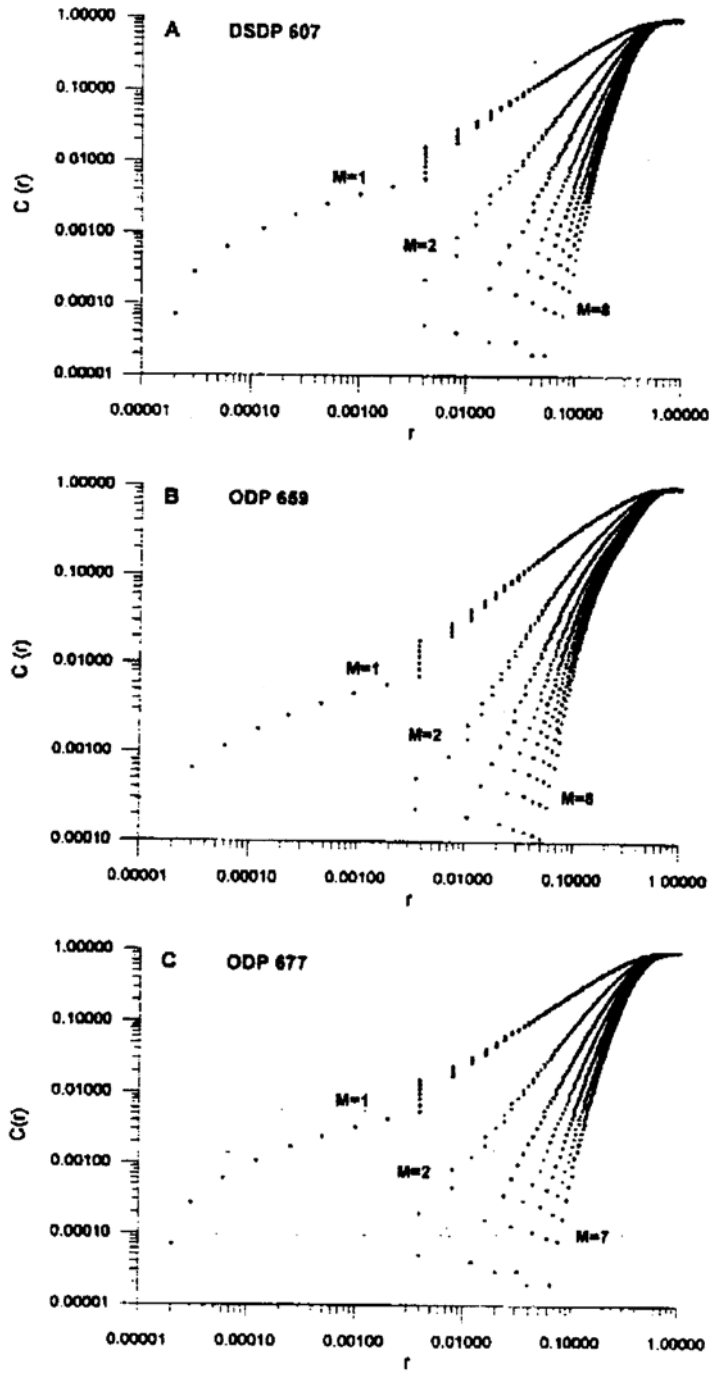

Fig. 3. Correlation integrals of the investigated time series, calculated with $M = 1, 2, \ldots$. Because of the double-logarithmic scale linear regions represent power-law dependences. For large values of r, $C(r)$ saturates because of the limited size of the embedding space (corresponding to the limited range of values of the time series). (A-D) For very small values of r, the power-law dependence is disturbed by the noise of the experimental data. The lower bound, r_L, of the scaling region, should orientate to the experimental noise strength which is in the order of (A) $r = 0.04$, (B) $r = 0.04$, (C) $r = 0.04$, (D) $r = 0.06$ (see text).

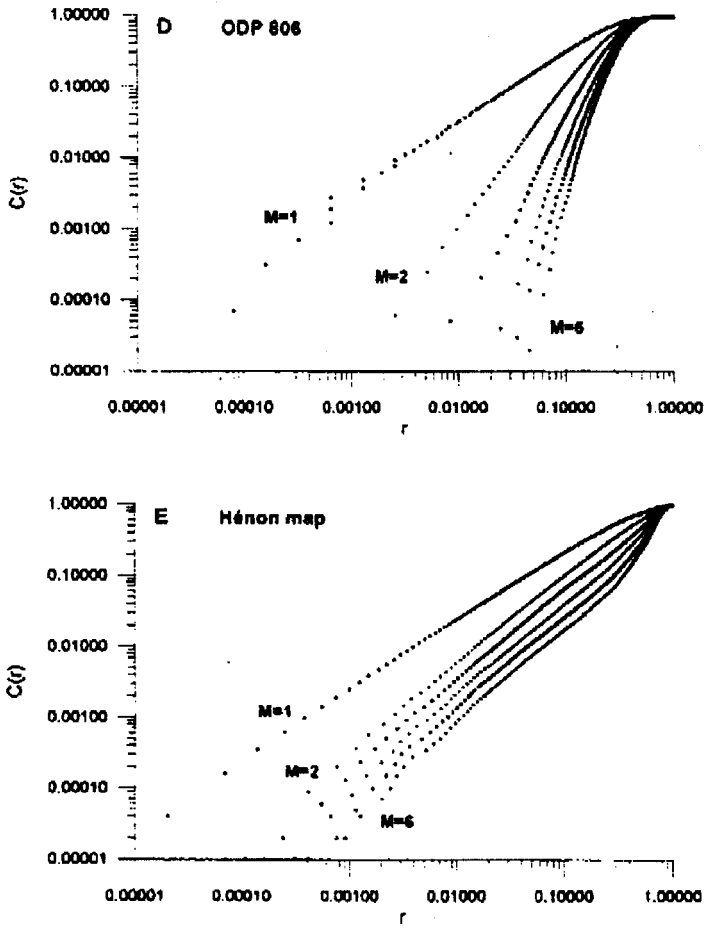

Fig. 3. Continued.

(1) To have a broad fit region for statistical reasons (Eckmann and Ruelle, 1992, see the next subsection).

(2) To be above a typical value of the experimental noise strength (Ben-Mizrachi et al., 1984). Considering that the distances $\|Y(i) - Y(j)\|$ are measured with the maximum norm, $r_L \approx \epsilon_x\sqrt{2}$ results (the values of the noise strength for each experimental time series, considering the normalization of the distances, r, (see above) are given in the caption of Figs. 3A–D). Although the values of the estimated parameters do not strongly depend upon r_L (Mudelsee and Stattegger, 1994) we obtain the best results using this recommendation.

(3) To have an optimum value for the goodness-of-fit. This measure must be independent of the number n_{fit} of fit points. Therefore, we use the ratio $\chi^2/(n_{\text{fit}} - 2)$.

(4) A proper visual linearity within the fit region when plotted on a double-logarithmic scale.

As all four aims cannot be fulfilled at the same time, an interactive procedure (evaluating a fit region—regression—judging the result—evaluating a new fit region—. . .) is applied.

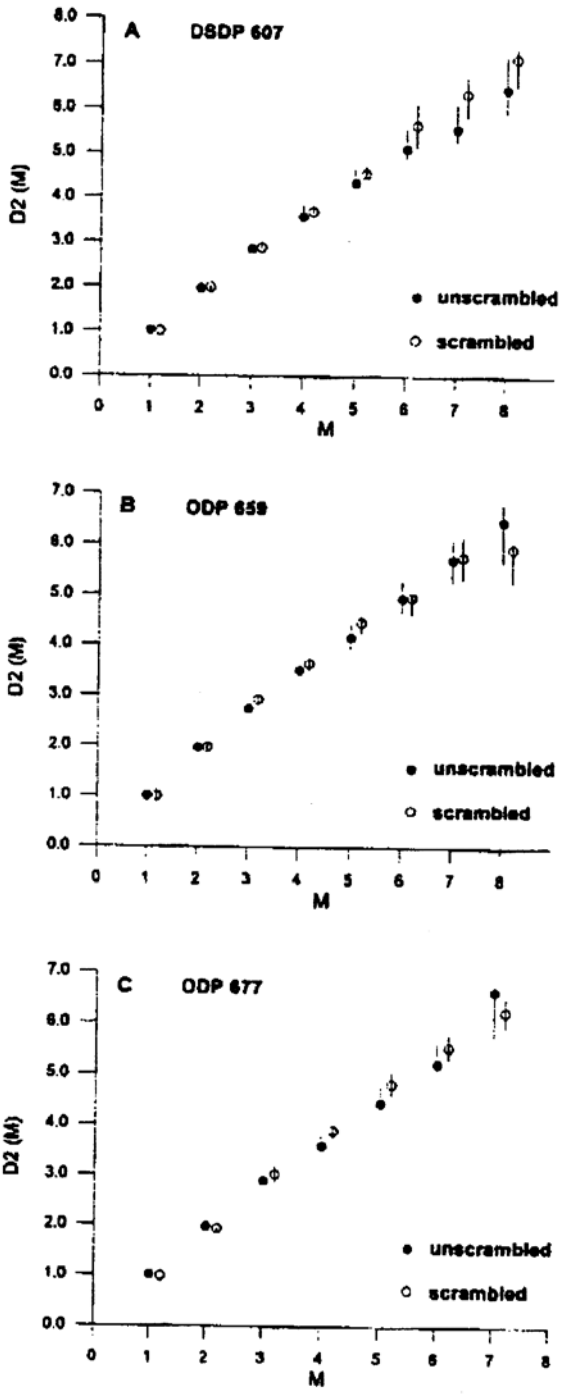

Fig. 4. Dependence of the estimated correlation dimension, $D_2(M)$, on the embedding dimension, M. (A-D) No saturation behavior is observed. The difference to the result from the scrambled time series is small. (E) The Hénon map time series shows the expected saturation for $D_2(M)$ at values between 1.22 and 1.28. The difference to the result from the scrambled time series is large. Also shown is the saturation behavior for $D_2(M)$ calculated with linear least-squares fits to the logarithmically transformed points at values between 1.33 and 1.48.

The regression itself consists of nonlinear least-squares fits using the Gauss-Marquardt algorithm. As starting values for the parameters we use the results from linear regression for the logarithmically transformed points. As the minimizing function $\chi^2(a, D_2(M))$ has a simple form (as can be verified analytically), stopping rules are easily formulated. The standard deviation of the estimated parameter $D_2(M)$ is determined by Monte Carlo simulation (number of simulations = 100) of the original X-values of the equidistant time series. We use

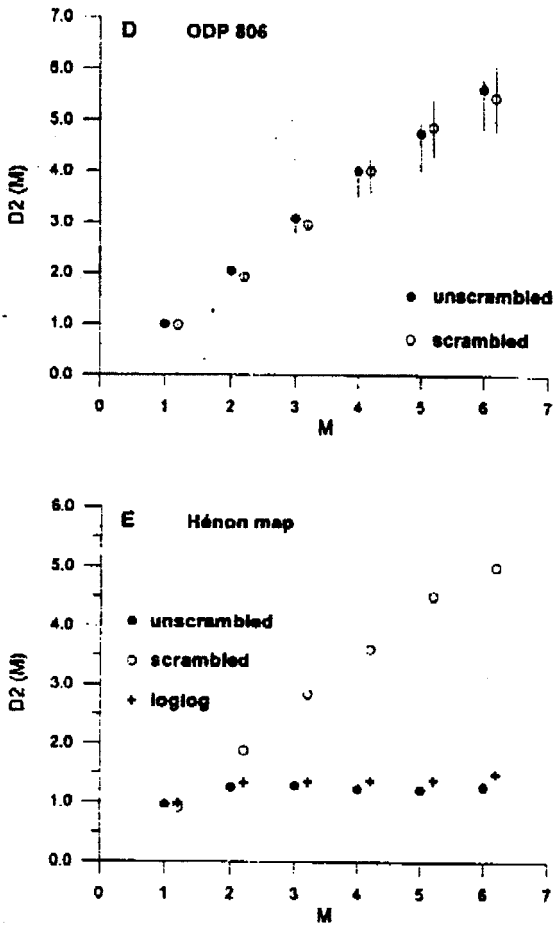

Fig. 4. Continued.

boundaries of $D_2(M)$ corresponding to the 95.45% minimum values of χ^2, which would mean 2-sigma errors in the case of normally distributed values. However, the bounds for $D_2(M)$ are uneven (Figs. 4A–D), indicating a nonnormal distribution. The Monte Carlo simulations take the greatest amount of computing time. The regression calculations are carried out using modified routines from Press et al. (1989).

We think that nonlinear fits are a methodical improvement of the Grassberger-Procaccia algorithm. We consider that there might be additional improvements in design of the regression step; for example, in the choice of points (r, C) to evaluate the correlation integral (see Seber and Wild, 1989, Chapters 3 and 5).

Influence of the Number of Data Points

As stated above, Eckmann and Ruelle (1992, page 186) gave a relation for the maximum sensible value of $D_2(M)$ dependent on the number of data points N of the time series. However, as we think that a factor of 1/2 was lost when moving from their formula (4) to formula (5) we quote their result (their formula (6)) with "$N/2$" instead of "N":

$$D_{2,\max} = 2 \log (N/2) / \log (1/\rho)$$

where ρ denotes the portion of the fit range with respect to the whole range of distances, r. A requirement that is roughly fulfilled in our application is that ρ should be in the order of 0.1 for statistical reasons (Eckmann and Ruelle, 1992). Considering the differences in N of our time series (Table 1), we find $D_{2,\max}$ to be in the order of 5. It means that our statement about the dimensionality of the paleoclimatic system is limited by at least this value. If we find no saturation behavior for $D_2(M)$ below 5 we do not increase M further and the calculations are stopped.

Stochastic Time Series

A very large number of influencing variables (i.e., noise processes) corresponds to a very high dimension of the original phase space, so the saturation behavior of $D_2(M)$ should then occur only for very large values of M. Hence, a time series generated by a white noise process does not show saturation (e.g., Schuster, 1989, p. 128–129). However, time series generated by a simple class of colored noise do show saturation (Osborne and Provenzale, 1989). We consider that this finding does not influence *rejections* of supposed low-dimensional systems.

In order to compare the behavior of $D_2(M)$ for the five investigated time series we also calculate $D_2(M)$ for the "scrambled" time series (Scheinkman and LeBaron, 1989). From a time series a "scrambled" time series is generated by randomly sampling from the original data set with replacement. A low-dimensional chaotic time series would produce a curve $D_2(M)$ that is less than $D_2(M)$ from the scrambled time series (Eckmann and Ruelle, 1992).

RESULTS

The results are shown in Fig. 4. In the case of the unscrambled Hénon map time series, the saturation behavior of $D_2(M)$ is clearly visible, whereas no saturation is observed for the scrambled time series (Fig. 4E). The saturation value found in our application (1.22–1.28) corresponds closely to the published value of $D_2 = 1.25 \pm 0.02$ (Grassberger and Procaccia, 1983). Further, $D_2(M)$ calculated with double-log plots and linear regression shows saturation; however, the saturation value is significantly higher (1.33–1.48), confirming the findings of Mudelsee and Stattegger (1994). We explain the fact that we find, using nonlinear regression, about the same value as Grassberger and Procaccia (1983) (who used double-log plots and linear regression) by the much greater number of data points in their time series (20000 in comparison to 1000 in our paper). This might have resulted in the assumed bias in the estimated value of D_2 (see above) becoming negligible.

In the case of the four experimental oxygen isotope time series no saturation is observed up to the maximum sensible value for D_2(M) of about 5 (Figs. 4A–D). The experimental time series cannot be distinguished from the scrambled time series by the algorithm. (In case of the ODP 659 time series, the same result had previously been quoted in Mudelsee and Stattegger (1994), where linear interpolation was used and commercial software for the nonlinear regression applied.)

CONCLUSIONS

One artificial, low-dimensional chaotic time series and four paleoclimatic time series have been analyzed with the Grassberger-Procaccia algorithm in order to investigate whether the paleoclimatic time series exhibit a low-dimensional chaotic behavior. As methodical improvements we inserted the Akima-subspline interpolation method as well as the nonlinear regression method.

The low dimensionality of the artificial time series was confirmed for a comparably small number of data points, supporting our insertion of nonlinear regression. However, if one is not interested in an exact value of the dimension but would prefer to know whether the time series is low-dimensional, then the linear regression on the logarithmically transformed points is also applicable.

The paleoclimatic time series (marine oxygen isotope records) are expected to reflect global climate variability on time scales ranging from about 2–5 Ma to 3–4 ka. This expectation is strengthened by the fact that the time series, originating from various locations, show the same results. For all four times series no saturation behavior of the estimated correlation dimension $D_2(M)$ was observed up to $D_2(M) \approx 5$. We infer that the investigated climate system is governed by five or more independent influencing variables. Statements about higher dimensions demand greater data sizes in order to reconstruct the original phase space.

This finding is of importance for the modeling of the corresponding paleoclimatic system: the global Plio-/Pleistocene climate system is driven externally by Milankovitch forcing with variations in eccentricity, obliquity, and precession. In the sedimentary records this external forcing is documented as well as the internal response of the climatic system. Investigating this response, we plan to test the assumption that not the whole spectrum of climate variability is due to nonlinearly interacting variables but that rather some harmonic components (discrete frequencies) exist. Harmonic components presumably should correspond to Milankovitch frequencies. By filtering out corresponding variability from the time series, it should be possible to single out the response of the Earth's climatic system to the orbital forcing. GRAPE-density measurements and magnetic susceptibility measurements will complete the paleoclimatic database. These records typically show data sizes one magnitude higher than

oxygen isotope records, they are expected to be more favorable in estimating higher dimensions.

ACKNOWLEDGMENTS

We gratefully acknowledge Wolfgang H. Berger and Memorie K. Yasuda, both at Scripps Institution of Oceanography, La Jolla, Maureen E. Raymo, MIT, Cambridge, and Ralf Tiedemann, GEOMAR, Kiel, for providing us with data material. Wolfgang H. Berger and Walter Schwarzacher made helpful and valuable review comments. Patrick S. Dingle and John O'Connor helped in refining the English of the manuscript. Manfred Mudelsee is working on his doctoral thesis within the Graduiertenkolleg "Dynamik globaler Kreisläufe im System Erde" at Kiel University which is funded by the Deutsche Forschungsgemeinschaft.

REFERENCES

Ben-Mizrachi, A., Procaccia, I., and Grassberger, P., 1984, Characterization of Experimental (Noisy) Strange Attractors: Phys. Rev. A, v. 29, p. 975–977.

Berger, A. L., 1992, Astronomical Theory of Paleoclimates and the Last Glacial-Interglacial Cycle: Quat. Sci. R., v. 11, p. 571–581.

Berger, W. H., Bickert, T., Schmidt, H., and Wefer, G., 1993, Quaternary Oxygen Isotope Record of Pelagic Foraminifers: Site 806, Ontong Java Plateau, *in* W. H. Berger, L. W. Kroenke, L. A. Mayer et al., eds., Proc. ODP, Sci. Results, v. 130: Ocean Drilling Program, College Station, Texas, p. 381–395.

Berger, W. H., Yasuda, M. K., Bickert, T., Wefer, G., and Takayama, T., 1994, Quaternary Time Scale for the Ontong Java Plateau: Milankovitch Template for Ocean Drilling Program Site 806: Geology, v. 22, p. 463–467.

Ding, M., Grebogi, C., Ott, E., Sauer, T., and Yorke, J. A., 1993, Estimating Correlation Dimension from a Chaotic Time Series: When Does Plateau Onset Occur?: Physica D, v. 69, p. 404–424.

Eckmann, J.-P., and Ruelle, D., 1992, Fundamental Limitations for Estimating Dimensions and Lyapunov Exponents in Dynamical Systems: Physica D, v. 56, p. 185–187.

Engeln-Müllges, G., and Reutter, F., 1993, *Numerik-Algorithmen mit FORTRAN 77-Programmen*, 7th Ed.: BI Wissenschaftsverlag, Mannheim Leipzig Wien Zürich, 1245 p.

Grassberger, P., 1986, Do Climatic Attractors Exist?: Nature, v. 323, p. 609–612.

Grassberger, P., 1987, Grassberger replies: Nature, v. 326, p. 524.

Grassberger, P., and Procaccia, I., 1983, Characterization of Strange Attractors: Phys. Rev. L., v. 50, p. 346–349.

Hays, J. D., Imbrie, J., and Shackleton, N. J., 1976, Variations in the Earth's Orbit: Pacemaker of the Ice Ages: Science, v. 194, p. 1121–1132.

Hénon, M., 1976, A Two-Dimensional Mapping with a Strange Attractor: Comm. Math. P., v. 50, p. 69–77.

Maasch, K. A., 1989, Calculating Climate Attractor Dimension from $\delta^{18}O$ Records by the Grassberger-Procaccia Algorithm: Clim. Dynam., v. 4, p. 45–55.

Mix, A. C., 1992, The Marine Oxygen Isotope Record: Constraints on Timing and Extent of Ice-

Growth Events (120–65 ka), *in* P. U. Clark and P. D. Lea, eds., *The Last Interglacial-Glacial Transition in North America:* Geol. Soc. America, Spec. Paper, 270, p. 19–30.

Mudelsee, M., and Stattegger, K., 1994, Application of the Grassberger-Procaccia Algorithm to the $\delta^{18}O$ Record from ODP Site 659: Selected Methodical Aspects, *in* J. H. Kruhl, ed., *Fractals and Dynamic Systems in Geoscience:* Springer-Verlag, Berlin, Heidelberg, New York, p. 399–413.

Newhouse, S., Ruelle, D., and Takens, F., 1978, Occurrence of Strange Axiom A Attractors Near Quasi Periodic Flows on T^m, $m \geq 3$: Comm. Math. P., v. 64, p. 35–40.

Nicolis, C., and Nicolis, G., 1984, Is There a Climatic Attractor?: Nature, v. 311, p. 529–532.

Osborne, A. R., and Provenzale, A., 1989, Finite Correlation Dimension for Stochastic Systems with Power-Law Spectra: Physica D, v. 35, p. 357–381.

Packard, N. H., Crutchfield, J. P., Farmer, J. D., and Shaw, R. S., 1980, Geometry from a Time Series: Phys. Rev. L., v. 45, p. 712–716.

Press, W. H., Teukolsky, S. A., Vetterling, W. H., and Flannery, B. P., 1989, *Numerical Recipes (FORTRAN Version)*: Cambridge University Press, Cambridge, 702 p.

Raymo, M. E., 1992, Global Climate Change: A Three Million Year Perspective, *in* G. J. Kukla and E. Went, eds., *Start of a Glacial, NATO ASI Series*, Vol. I 3: Springer-Verlag, Berlin, Heidelberg, New York, p. 207–223.

Raymo, M. E., Ruddiman, W. F., Backman, J., Clement, B. M., and Martinson, D. G., 1989, Late Pliocene Variation in Northern Hemisphere Ice Sheets and North Atlantic Deep Water Circulation: Paleoceanography, v. 4, p. 413–446.

Ruddiman, W. F., Raymo, M. E., Martinson, D. G., Clement, B. M., and Backman, J., 1989, Pleistocene Evolution: Northern Hemisphere Ice Sheets and North Atlantic Ocean: Paleoceanography, v. 4, p. 353–412.

Ruelle, D., 1981, Chemical Kinetics and Dynamical Systems, *in* A. Pacault and C. Vidal, eds., *Nonlinear Phenomena in Chemical Dynamics*: Springer-Verlag, Berlin, Heidelberg, New York, p. 30–37.

Scheinkman, J. A., and LeBaron, B., 1989, Nonlinear Dynamics and Stock Returns: J. Business, v. 62, p. 311–337.

Schulz, M., 1994, Spektralanalyse nicht äquidistanter paläoklimatischer Zeitreihen: SPECTRUM—ein Turbo Pascal Programm: M. Sc. Thesis, Universität Kiel, 182 p.

Schuster, H. G., 1989, *Deterministic Chaos*, 2nd Ed.: VCH, Weinheim, 270 p.

Schwarzacher, W. 1993, *Cyclostratigraphy and the Milankovitch Theory: Developments in Sedimentology*, Vol. 52: Elsevier, Amsterdam, 225 p.

Seber, G. A. F., and Wild, C. J., 1989, *Nonlinear Regression*: John Wiley & Sons, New York, 768 p.

Seibold, E., and Berger, W. H., 1993, *The Sea Floor*, 2nd Ed.: Springer-Verlag, Berlin, Heidelberg, New York, 356 p.

Shackleton, N. J., and Hall, M. A., 1989, Stable Isotope History of the Pleistocene at ODP Site 677, *in* K. Becker, H. Sakai et al., eds., *Proc. ODP, Sci. Results*, Vol. 111: Ocean Drilling Program, College Station, Texas, p. 295–316.

Shackleton, N. J., Berger, A. L., and Peltier, W. R., 1990, An Alternative Astronomical Calibration of the Lower Pleistocene Timescale Based on ODP Site 677: Trans. Roy. Soc. Edinburgh: Earth Sci., v. 81, p. 251–261.

Theiler, J., 1986, Spurious Dimension from Correlation Algorithms Applied to Limited Time-Series Data: Phys. Rev. A, v. 34, p. 2427–2432.

Tiedemann, R., 1991, Acht Millionen Jahre Klimageschichte von Nordwest Afrika and Paläo-Ozeanographie des angrenzenden Atlantiks: Hochauflösende Zeitreihen von ODP-Sites 658-661: Berichte—Reports, Geol.—Paläont. Inst. Univ. Kiel, 46, 190 p.

Tiedemann, R., Sarnthein, M., and Shackleton, N. J., 1994, Astronomic Timescale for the Pliocene Atlantic $\delta^{18}O$ and Dust Flux Records of ODP Site 659: Paleoceanography, v. 9, p. 619–638.